CHAPTER 17

Thermonuclear Reactions: The Beginning and the Future

Contents

Hydrogen, deuterium and most of the helium atoms in the universe are believed to have been created some 20 billion years ago in a primary formation process referred to as the *Big Bang*, while all other elements have been formed — and still are being formed — in nuclear reactions in the stars. These reaction processes can only be understood in an astrophysical context, as briefly outlined in this chapter, which also describes how nuclear science has provided much understanding about the universe, our solar system and our planets. Because the simplest fusion reactions, which created the lightest elements, could in the future provide us with an almost unlimited source of energy in controlled thermonuclear reactors, this is also discussed here.

17.1. Observations from space probe Earth

17.1.1. *Our place in the Universe*

The stars we directly can see all belong to our Galaxy, the *Milky Way*, which is a spiral galaxy, about 30 kpc across and about 1 kpc thick. The kpc, kiloparsec, is the common astronomical unit of distance; 1 parsec is 3.1×10^{16} m, or 3.26 light years, ly. Thus light travels across our galaxy in about 100 000 y. The Milky Way contains some 200×10^{9} stars, and interstellar dust and gas (~ 200 pc thick) which spreads out to a diameter of about 50 kpc (hot gas atoms, the *halo*). Our sun is located at the outer edge of one of the spiral arms, about 8.5 kpc from the galactic center. The dust limits the sight towards the center to only a few kpc; without this dust the Galaxy center would shine equally bright as our sun. The stars in our Galaxy move tangentially around its center with angular velocities increasing closer to the center, indicating the existence of a heavy central object, called Sagittarius (Sgr) A*.

The Milky Way belongs to the *Local Group*, a cluster of some 20 galaxies which include i.a. the Large Magellanic Cloud, our nearest galaxy, 50 kpc away and the Andromeda galaxy, 650 kpc away. The Local Group is part of the larger *Virgo super-cluster*. The universe contains some 10^{10} galaxies. The galaxies only fill a fraction of space, < 5%, the rest appears void of matter.

In the 1930s Hubble discovered that galaxies on the whole are equally distributed in all directions of space as observed from the earth. Thus space — on a large scale — seem to be isotropic. This idea of uniformity of the universe is called *the cosmological principle*.

This information has been deduced from *celestial mechanics* (movements of bodies according to Newton's fundamental laws) and from spectroscopic analysis of light and other kinds of radiation. It has been found that the mass of our sun is 1.99×10^{30} kg (= 1 solar mass, $\mathbf{M}_\odot$). The mass of the Milky Way is $> 2 \times 10^{11}$ $\mathbf{M}_\odot$ about 10% of the mass is interstellar gas, and 0.1% is dust (typically particles with diameter 0.01 - 0.1 µm). The interstellar gas density varies considerably in our galaxy; in our part of space it varies from about 10^9 (in dark clouds) to 10^5 atoms m^{-3} (on the average ~ 1 atom cm^{-3}). Though it contains mainly H and He, also large rather complex molecules containing H, C (up to C_{15} molecules), N and O (including amino acids) have been discovered.

17.1.2. *Dark matter*

Astronomical models of the universe indicate that it will expand forever if the observed galaxies alone should account for the total mass of the universe. Almost 90% is missing of the mass needed for a slowing down and ultimately contracting universe. Most cosmologists believe that the mass of the observed galaxies is $\leq$ 10% of the mass of the universe, the main part consisting of "*dark matter*"; this includes interstellar and intergalactic matter, *neutron stars*, "*black holes*" and other little known sources of radiation, like quasars, whose masses are unknown.

From mechanics and Newton's gravitational law one can calculate the velocity needed for a body, m_x, to escape the gravitational pull of a larger mass, m, where $m_x \ll m$. For example, if m is the earth's mass (5.94×10^{24} kg), a rocket (mass m_x) must have a velocity of about 11 km/s to escape from the earth's surface (the *escape velocity*, v_e). Conversely, for a given velocity, v_e, one can calculate the mass and size of the large body needed to hamper such an escape. A body with our solar mass, $\mathbf{M}_\odot$, but a radius of only 3 km, requires an escape velocity $> 3 \times 10^{10}$ m/s. Thus not even light will escape such a body, which therefore is termed *black hole*. Though we cannot observe the black holes directly, some secondary effects can be observed.

Astronomical observations of star movements support the existence of black holes. For example, from movements of stars close to our galactic center, it is believed that a black hole is located at SgrA* in the center of the Milky Way, with a mass $> 3 \times 10^6\, \mathbf{M}_\odot$. The radius of such a hole would be of the same size as that of our sun. The density of matter in the hole would be several million times the density of our sun (average value for the sun is about 1400 kg/m^3). Obviously matter cannot be in the same atomic state (i.e. nuclei surrounded by electrons) as we know on earth. Instead we must assume that the electron shells are partly crushed; we refer to this as *degenerate matter*, because the electron quantum rules, Tables 11.1 - 11.2, cannot be upheld. For completely crushed atoms, matter will mainly consist of compact nuclei. For example, for calcium the nuclear density is $\sim 2.5 \times 10^{17}$ kg/m^3 (cf. Fig. 3.4).

Even if black holes are given a considerable portion of the missing mass, this will not be enough. However, a very recent discovery may provide the "needed" mass: Detailed analysis of the variation in luminosity (a factor of about 2.5) for some 10 million double stars in the Large Magellanic Cloud, gives support for the existence of nearby "*gravitational microlenses*", which are believed to be unborn stars (so-called *brown dwarfs*, §17.3) of sizes $\sim 10\, \mathbf{M}_\odot$. When such a dark object passes the line of sight to a distant star it acts as a focusing lens for the light, thereby temporarily increasing that star's apparent luminosity. As these gravitational microlenses seem to be especially abundant in the halo of our galaxy (and presumably in halos of other galaxies), they — together with neutron stars and black holes — could account for the 90% of "missing dark matter" required for an ultimately contracting universe.

17.1.3. *Light, energy flux and the Hubble law*

Spectral analysis of the light received from astronomical objects have provided us with information of their (surface) *temperature* (from their continuous spectrum) and outer *chemical composition* (from identification of spectral line frequencies), while bolometric measurements have given their *luminosity* (energy flux density, F Wm^{-2}). In 1911 Hertzsprung and Russell discovered that if the luminosity and color (or temperature) of stars in different galaxies were compared with similar type of stars in the Milky Way, the stars become distributed according to a certain pattern, the so-called *Zero Age Main Sequence* (ZAMS) of stars; it is believed that most stars in their evolution follow the diagram beginning at the lower right side, along the main sequence into the red giant phase, then

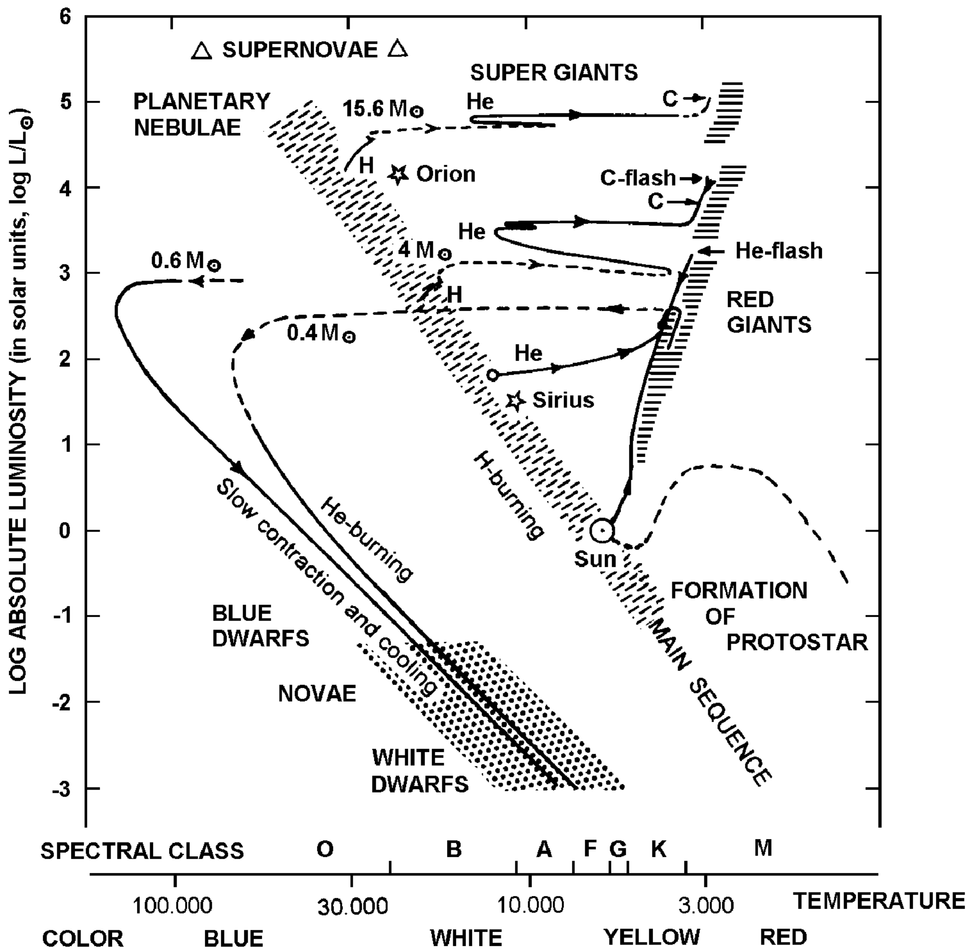

FIG. 17.1. HR-diagram showing surface temperature, spectral class and color for stars born on the main sequence as a function of their absolute luminosity relative to the solar mass $M_{\odot}$.

to the left and down, decreasing in size and temperature to end as blue or white dwarfs. *Hertzsprung-Russell* (*HR-*)*diagrams*, like the one in Figure 17.1, are valid for stars of about 0.7 – 70 $\mathbf{M}_{\odot}$: from such diagrams conclusion can be drawn about the *size* (or *mass*) and *relative age* of the star, as it is assumed that stars of a given mass follow the same sequence as they age. The apparent luminosity, *F*, which we observe with our telescopes, is related to the *absolute luminosity*, *L**, i.e. the total *energy flux* in all directions from a star, by the relation

$$F = L^* / 4 \pi d^2 \tag{17.1}$$

where *d* is the *distance* from the star. The historical classification of stars into *brightness classes* is now usually replaced by their relative (or apparent) *magnitude*, m^*, defined as $m^* = -2.5 \log(F/F_0)$, where F_0 is a reference flux density.

Hubble discovered that all galaxies, except for those in the Virgo, show a *spectral red-shift* (i.e. increased distance between known frequency lines). This is assumed to be a Doppler effect due do that the objects move away from us (compare the lowering of the pitch from the horn of a train moving away from us). The red shift z is

$$z = (\lambda - \lambda_o)/\lambda_o = \mathbf{H}\, d / \mathbf{c} \tag{17.2}$$

where **H** is the *Hubble constant*. For *velocities* $v \ll \mathbf{c}$, the relation becomes $z = v/\mathbf{c}$, hence

$$v_r = \mathbf{H}\, d \tag{17.3}$$

which is the common expression of the *Hubble law*; v_r is the *radial velocity*. If the red shift is plotted against the apparent magnitude of the brightest star in a large number of galaxies it is seen to increase with decreasing luminosity, which is interpreted so as that more distant (faintest) galaxies move away faster from us than the closer ones. Except for the galaxies in the Local Group, all galaxies recede from us with velocities up to 20 000 km/s; hence it is concluded that *the universe expands*.

17.1.4. *Determination of ages*

If the universe is expanding, the galaxies were once much closer to each other. If the rate of expansion has been unchanged, the inverse of the Hubble constant, $\mathbf{H}^{-1}$, would represent the *age of the universe*.

In (17.3) v_r is the radial velocity of a galaxy at distance d from us. But velocity is just distance divided by time; i.e. $v_r = d / t_o$, where t_o is the time the movement (expansion) has gone on, assuming a constant speed. Thus,

$$d / t_o = \mathbf{H}\, d \tag{17.4a}$$

or

$$t_o = 1 / \mathbf{H} \tag{17.4b}$$

t_o is only an upper limit of the age of the universe, because we have all reasons to believe that the movement has slowed down due to gravitational pull. According to present estimates a **H**-value of 0.05 – 0.1 $\mathrm{m\,s^{-1}\,pc^{-1}}$ corresponds to an age of 10 – 20 Gy (gigayears, 10^9 years, or *eons*). Cosmologists also give the age in the "scale factor" $(1 + z)$-values, i.e. red-shift values; e.g. we would observe a z-value of 10 for an object about one billion years old from the formation of the universe.

The *lifetime of a solar system* can be estimated from its composition and energy production. The average surface temperature of our sun is 5780 K while that of its center is about 1.5×10^7 K. The energy production rate is 3.76×10^{26} J $\mathrm{s^{-1}}$ and is assumed to have been relatively constant since the formation of the sun about 5 eons ago. The energy production is so immense that gravitation alone cannot account for it, leading to the conclusion that the main solar energy source is not gravitational but nuclear. This is strongly supported by the cosmic abundance of the elements.

The high temperature allows hydrogen to fuse into helium by the reaction

$$4\,{}^1\mathrm{H} \rightarrow {}^4\mathrm{He} + {}^*2\beta^+ + 2e^{-*} + 2\nu_e \quad Q = 24.7 + 2 \times 1.02 = 26.7\ \mathrm{MeV} \qquad (17.5)$$

(neutrinos take away 0.06 MeV; see also §17.3). One calculates that in 5 eons $\sim 9 \times 10^{28}$ kg ^{1}H was consumed, which is $\sim 5\%$ of the suns current content of ^{1}H. H-burning is assumed to be the main source of nuclear energy in a star of mass m. It is possible to calculate the time it takes to consume all available hydrogen; this is referred to as *the nuclear time scale*. From (17.5) one finds that about 0.70% of the hydrogen mass is converted into energy. As only about 10% of the hydrogen can be consumed before other more rapid evolutionary mechanisms set in (see below), the *nuclear lifetime*, t_n, is

$$t_n = 0.0070 \times 0.10 \times m\,\mathbf{c}^2 / L \qquad (17.6)$$

which, for our sun ($m = \mathbf{M}_\odot$), gives a value of $\sim 10^{10}$ years, i.e. 10 eons.

The *age of matter* can be determined from its content of radioactive (and sometimes also stable) isotopes, as described in Chapter 5. From analyzes of lunar and meteoritic samples the age of the solar system has been calculated to be about 4.7 eons. The spectra of the light from some stars in our galaxy show the existence of relatively short lived elements like technetium (longest lived isotope has a half-life of 4.1×10^6 y). Because these elements cannot be formed in the main sequence stars, as we shall see later, they must have been accumulated "recently" from interstellar matter, indicating that these stars are rather young. From HR-diagrams, stars in our galaxy appears to be have ages from < 0.1 to > 6 eons. Thus the evidence is that the formation of stars has gone on for a long period of time and is still occurring.

17.1.5. *Elemental composition*

Figure 17.2 shows the *relative abundance* of the elements of the universe and of the earth. The abundances are approximate, as a consequence of the difficulties in their assessment and limitations of experimental techniques. The abundances in the universe (based on spectral measurements on stars and interstellar matter) are used as a refinement of data obtained for the solar system. Stellar light is divided in spectral classes depending on the surface temperature of the star, see Fig. 17.1. The various classes (Harvard Spectral Classification) show lines of the elements as listed below in approximately decreasing intensity:

O	He^+, N^{2+} and Si^{3+}; weak H lines
B	He, $Si^{+,2+}$, O^+, Mg; more H than in Class O
A	Strong H; Mg^+, Si^+, Fe^+, Ti^+, Ca^+ and some other metals
F	H weaker than Class A; also Ca^+, Fe^+, Cr^+ and other metals
G	Lines of ionized metals; less H; also CH and hydrocarbons
K	Lines of neutral metals; also CH present
M	Lines of neutral metals; also molecular bands from C_2, CN, CH, TiO, ZrO, etc

Some stars are labeled chemically peculiar (CP-stars) because their light spectra are different from most stars in the main sequence, e.g. they have very strong lines of rare

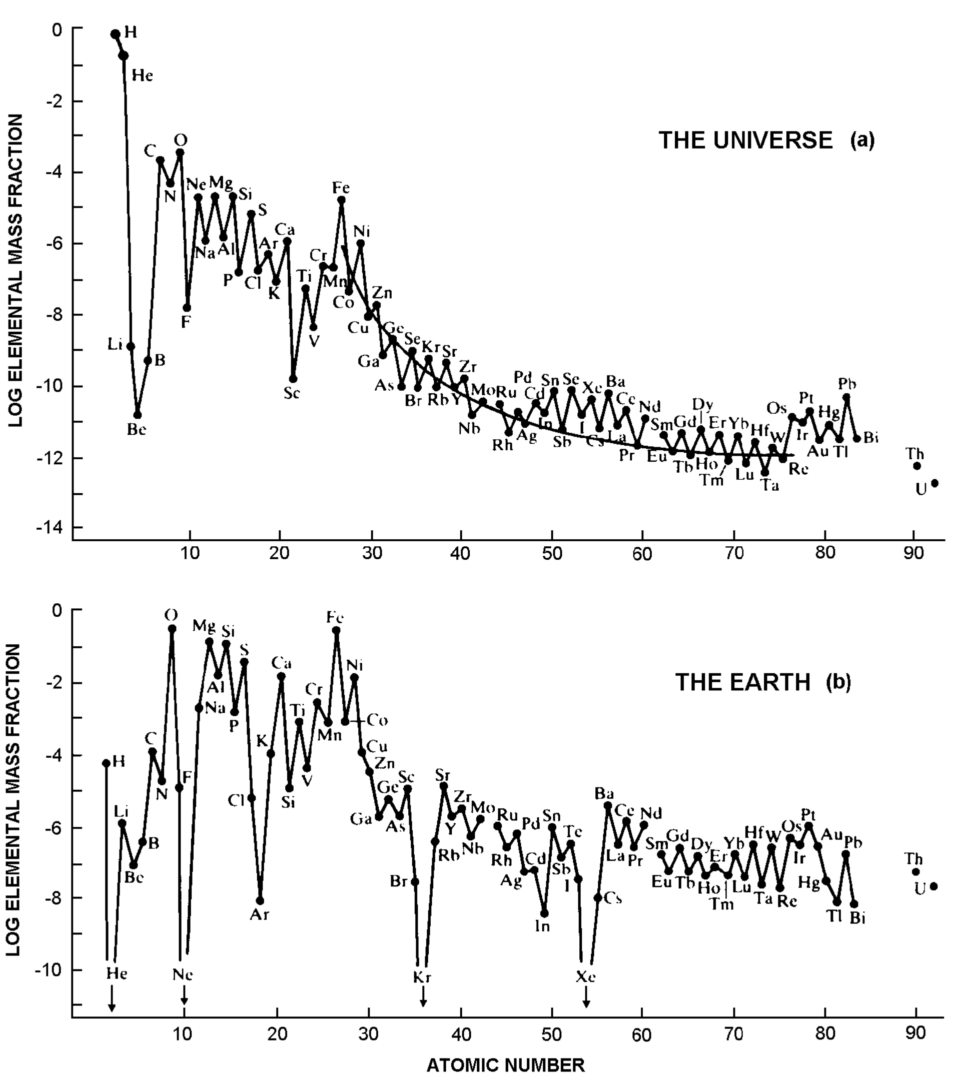

FIG. 17.2. Relative abundances of the elements in the universe and the earth. (From Cox.)

earth or heavy elements. Strong lines are assumed to reflect that these elements have been moved up from the core by heavy turbulence. The Hubble Space Telescope (HST), which was placed in orbit around the earth in 1990, has allowed detailed spectroscopic analysis of CP-stars. For example in X-Lupi, high concentrations of heavy metals like Hg, Ru and Pt have been discovered; and 100% of the mercury is ^{204}Hg, while the solar abundance of that isotope is only 7%.

The abundance data in Figure 17.2 show some regularities:

(i) H and He are the dominating elements in the universe ($>$ 99 %),

(ii) the abundances show a rapid, exponential decrease with increasing Z,

(iii) there is a pronounced abundance peak $Z = 26$ (Fe), and minor peaks at 6 and 8 (C and O),

(iv) elements of even atomic number are more abundant than their neighbors of odd atomic number.

Further, a study of isotopic abundances shows:

(a) for the lightest elements, isotopes of masses which are multiples of 4 show the highest abundances, indicating their formation through fusion of He-atoms;

(b) for isobars lighter than $A \approx 70$ (corresponding to $Z \approx 28$) the most proton rich (or most neutron deficient) isobar is the most abundant, while the opposite goes for isobars with $A > 70$, indicating two different modes of synthesis for elements lighter than and heavier than $Z \approx 28$;

(c) elements that have N and Z values close to the magic numbers (Ch. 11) are more abundant then neighboring ones, further supporting the idea of elemental formation through nuclear processes.

From these and additional observations Burbidge, Burbidge, Fowler, and Hoyle ("B^2FH") and others have developed a model for elemental formation in the universe, which is the basis for the subsequent discussion.

17.1.6. *Microwave radiation and the Big Bang*

In 1965 it was discovered that low energy microwave radiation (at 7.35 cm uncorrected) reaches us from all directions in space (about 400 photons cm^{-3}). This is referred to as the *cosmic background radiation* whose wavelength corresponds to radiation from a black body of temperature 2.7 K (about 0.0003 eV). Thermodynamic calculations show that this is the temperature reached after adiabatic expansion of a very hot cloud for some 10 billion years. The existence of such a background radiation was predicted by Gamow decades before in a cosmological hypothesis referred to as the *Big Bang model*. Recent measurements have shown that the intensity of this radiation varies slightly ("ripples") in different directions in space.

The Big Bang hypothesis requires an instantaneous beginning of our universe at a point to which all energy (in the Planck-Einstein matter-radiation-energy concept; Ch. 12) is concentrated. Ordinary nuclear reactions cannot model this beginning and we must turn to particle physics for information (Ch. 10).

In the following we describe the formation of the universe and the elements according to the so-called *Standard Model of Stellar Evolution*, which is based on the models originally developed by Bethe and Weizsäcker in the 1930's for the reactions in the sun, and the Big Bang hypothesis for the formation of the universe as originally suggested in 1948 by Gamow, Alpher and Herman, and later developed by the B^2FH-group, Weinberg and others.

17.2. In the beginning of time

Around "time zero" the Universe consisted of an immensely dense, hot sphere of photons, quarks and leptons, and their antiparticles, in thermal equilibrium, particles being created by photons and photons created by annihilation of particles. The temperature must have been $\geq 10^{13}$K, but no light was emitted, because of the enormous gravitational force pulled the photons back. The system was supposed to be in a unique state with no repulsion forces. However, just as a bottle of supercritical (overheated) water can explode by a phase transition, so did the Universe, and time began. The Universe expanded violently in all directions, and as age and size grew, density and temperature fell.

A one hundreds of a second later all the quarks were gone, and the Universe consisted of an approximately equal number of electrons, positrons, neutrinos and photons, and a small amount of protons and neutrons; the ratio of protons to photons is assumed to have been about 10^{-9}. The temperature was about 10^{11}K and the density so high, about 4×10^6 kg m^{-3}, that even the unreactive neutrinos were hindered to escape.

The conditions can be partly understood by considering the relations

$$E \text{ (MeV)} = m\,\mathbf{c}^2 = 931.5\,\Delta M \qquad (3.3 \text{ and } 17.7)$$

which gives the energy required to create a particle of mass ΔM (E in MeV, ΔM in u), and

$$E \text{ (MeV)} = \mathbf{k}\,T = 8.61 \times 10^{-11}\,T \qquad (2.39 \text{ and } 17.8)$$

which gives the average kinetic energy of a particle at temperature T (K, Kelvin). As the photon energy of E (eV) corresponds to the wavelength λ (m) according to (5.1) – (5.2)

$$E \text{ (eV)} = \boldsymbol{h}\,\nu = \boldsymbol{h}\,\mathbf{c}\,/\,\lambda = 1.240 \times 10^{-6}\,/\,\lambda \text{ (m)} \qquad (17.9)$$

one can estimate that the creation of a proton or a neutron (rest mass 940 MeV) out of radiation requires a temperature of 1.1×10^{13} K, corresponding to a photon wave length of about 10^{-15} m, i.e. the size of a nucleon. At these temperatures nucleons are formed out of radiation, but are also disrupted by photons, leading to an equilibrium with about an equal number of protons and neutrons. At temperatures below the threshold formation energy, no nucleons are formed. However, it should be remembered that particles and radiation are distributed over a range of energies, according to the Boltzmann (cf. Fig. 2.3) and Planck distribution laws. Thus some formation (and disruption) of nucleons occurs even at lower temperatures.

In about 0.1 s the temperature is assumed to have decreased to 3×10^{10} K (corresponding to 2.6 MeV). Now, the equilibrium between protons, neutrons, electrons and neutrinos can be written

$$\text{p} + \nu \rightleftharpoons \text{n} + \text{e}^+ \quad Q = -1.80 \text{ MeV} \qquad (17.10a)$$

$$\text{n} + \nu \rightleftharpoons \text{p} + \text{e}^- \quad Q = 0.78 \text{ MeV} \qquad (17.10b)$$

The mass of the neutron exceeds that of the proton by a small margin of 0.00013885 u, corresponding to 1.29 MeV; thus reaction (a) requires energy, while reaction (b) releases energy. The formation of protons was therefore favored over neutrons, leading to 38% neutrons and 62% protons.

As temperature and density further decreased the neutrinos began to behave like free particles, and below 10^{10} K they ceased to play any active role in the formation sequence (matter became transparent to the neutrinos). The temperature corresponded then to ~ 1 MeV, i.e. about the threshold energy for formation of positron/electron pairs. Consequently they began to annihilate each other, leaving, for some reason, a small excess of electrons. Though neutrons and protons may react at this temperature, the thermal energies were still high enough to destroy any heavier nuclides eventually formed.

After 14 s the temperature had decreased to 3×10^9 K (0.27 MeV) and 3 min later to about 10^9 K ($<$ 0.1 MeV). Now, with the number of electrons, protons and neutrons about equal (though the universe mostly consisted of photons and neutrinos), some protons and neutrons reacted to form stable nuclides like deuterium and helium:

$$^{1}\text{H} + {}^{1}\text{H} \rightarrow {}^{2}\text{H} + {}^{*}\text{e}^{-} + \beta^{+*} + \nu_e \quad Q = 0.42 + 1.02 = 1.44 \text{ MeV} \tag{17.11}$$

This reaction is exothermic; however, for the ^{2}H to be stable, the temperature must decrease below the Q-value, i.e. to about 10^{10} K, and, in reality, to the much lower value of about 10^9 K, because of the high photon flux which may dissociate ^{2}H into 2 ^{1}H. Two deuterium atoms then fuse, probably in several steps as discussed below, to form He:

$$^{2}\text{H} + {}^{2}\text{H} \rightarrow {}^{4}\text{He} \quad Q = 23.85 \text{ MeV} \tag{17.12}$$

^{4}He is an extremely stable nucleus, not easily destroyed, as compared to nuclides with masses $>$ 4, whose binding energies (per nucleon) are only a few MeV (Fig. 3.3). As the universe expanded, the probability for particle collisions decreased, while the kinetic energy available for the fusion reactions was reduced. Therefore, the nucleon build-up in practice stopped with ^{4}He, leading to an average universal composition of 73% hydrogen and 27% helium. A very small amount of deuterium atoms was still left, as well as a minute fraction of heavier atoms, formed by the effects of the "Boltzmann tail" and "quantum tunneling" (see §17.4 and Fig. 17.3). The remaining free neutrons (half-life 10.4 min) now decayed to protons.

The situation about 35 minutes after time zero was then the following: Temperature was 3×10^8 K, density about 10^{-4} kg m^{-3}. The Universe consisted of 69% photons, 31% neutrinos, and a fraction of 10^{-9} of particles consisting of 72 – 78% hydrogen and of 28 – 22% helium, and an equivalent number of free electrons, all rapidly expanding in all directions of space.

It was still too hot for the electrons to join the hydrogen and helium ions to form neutral atoms. This occurred not until about 500 000 years later, when temperature had dropped to a few 1000 K. The disappearance of free electrons broke the thermal contact between radiation and matter, and radiation continued then to expand freely. An outside spectator would have observed this as a hugh flash and a rapidly expanding fireball. In the adiabatic expansion the radiation cooled further to the cosmic background radiation level of 2.7 K measured today.

The recent observation that the cosmic background radiation shows ripples in intensity in various directions of space indicates a slightly uneven ejection of matter into space, allowing gravitational forces to act, condensing the denser cloud parts into even more dense regions, or "islands", which by time separated from each other, leaving seemingly empty space in between. Within these clouds, or proto-galaxies, local higher densities lead to the formation of stars, as will be explained in next section.

17.3. Star ignition

The condensation of matter releases gravitational energy which is transformed into kinetic energy of the particles in the gas cloud, increasing temperature and pressure. As the density increases, radiation transport through the cloud becomes more difficult, leading to more rapid heating of the gas.

At some critical density, the *Chandrasekhar limit*, the hydrogen degenerates into H^+ ions and non-localized ("free") electrons (this is the *plasma state*). The ionization energy of H (13.6 eV) corresponds to an average kinetic particle energy of 160 000 K, eqn. (2.21), but because of the particle energy distribution (Fig. 2.4), degeneration begins already at lower temperature. Because the elimination of the electron shell leads to a pressure reduction, the gravitational forces cause an increased rate of condensation, with a further rise in temperature until eventually all the gas is ionized.

Because the temperature decreases from the center towards the shell, the light emitted from the center may be absorbed in outer layers. Thus the protostar may be invisible, but as it gradually heats up it begins to emit light. There are many such faint objects in our galaxy.

Depending on the mass of the contracting cloud, the star evolution follows different paths.

(i) For a cloud with $m < 0.08\ \mathbf{M}_\odot$, temperature and pressure never reach high enough values for hydrogen ignition and such "stars" will contract to planet-like *brown dwarfs*.

(ii) For masses $> 0.08\ \mathbf{M}_\odot$ fusion reactions begin when the core reaches $\geq 4\times10^6$ K. In Figure 17.1 we have indicated the birth of a star like our sun (1 $\mathbf{M}_\odot$) which appears initially as a red object in the sky, indicating a low surface temperature, but the luminosity slowly increases over a condensation time of $10^5 - 10^6$ y.

The Coulomb barrier for interaction of protons with each other is 1.1 MeV, eqn. (12.14). In the sun, density and temperature increases strongly from the surface towards the core. At a core temperature of 1.4×10^7 K, the average kinetic energy of a proton is only 1.8 keV (the most probable energy is 1.2 keV, § 2.6.2), while the fraction of protons with energies $\geq$ 1.1 MeV is only $\sim 10^{-398}$, eqn. (2.25). Formation of a ^{2}He nucleus from two protons is endothermic and will not occur by tunneling due to the lack of a driving force. On the other hand the reaction forming ^{2}H is exothermic. Hence, quantum mechanical tunneling can allow two protons to interact to form a ^{2}H nucleus according to (17.11) during the brief encounter of a scattering event even at energies $\ll$ 1.1 MeV. The reaction cross section is extremely small due to the involvement of the weak force and a change in spin for one of the nucleons ($\sim 10^{-47}$ barn at 1 MeV collision energy). Once deuterium has been formed it may fuse into helium. Thus the star has begun its "childhood" by burning hydrogen into helium: it has entered the Zero Age Main Sequence of stars. Stars with smaller masses enters lower on the Main Sequence, and evolves very slowly.

(iii) Stars with $0.08\ \mathbf{M}_\odot < m < 0.26\ \mathbf{M}_\odot$ are completely convective, leading to hydrogen burning to helium, until all hydrogen is exhausted, after which the star contracts to a *white dwarf*.

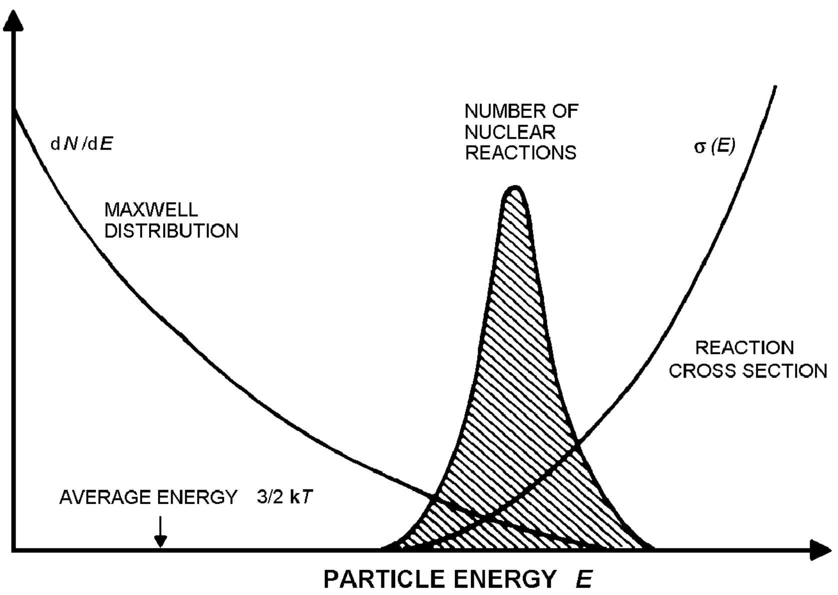

FIG. 17.3. Fusion reactions occurring in the shaded area, as a function of particle energy, showing Maxwell particle distribution and reaction cross section.

Other stars, with $m > 0.26\ \mathbf{M}_{\odot}$, evolve differently depending on their masses, as shown in Figure 17.1 and described in the following sections.

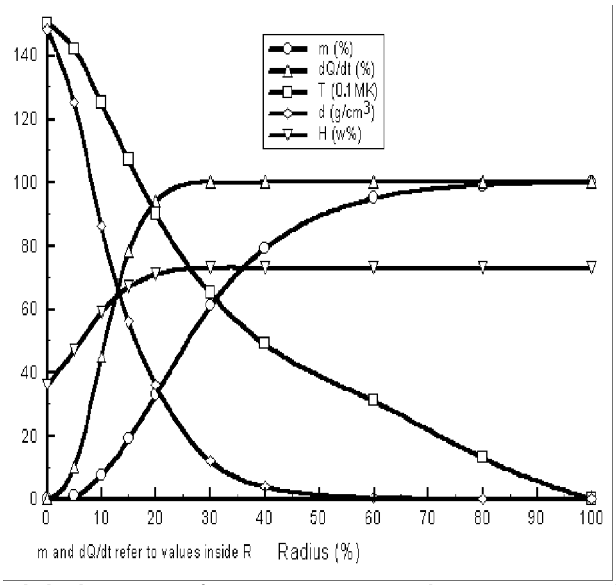

FIG. 17.4. Calculated composition of our sun (mass, energy production, temperature, density and hydrogen content) as function of the radius.

17.4. Fusion processes in stars

The elemental composition of our sun is about 73% hydrogen, 25% helium, and 2% carbon, nitrogen, oxygen, and other elements distributed as shown in Figure 17.2. In all, approximately 70 elements have been detected in the solar spectrum and there are reasons to believe that all the elements to uranium are present in our sun. Let us now consider the reactions for the formation of all these elements and the energy producing nuclear processes in our sun and other stars.

The present understanding of processes in the interior of stars is the result of combined efforts from many scientific disciplines such as hydrodynamics, plasma physics, nuclear physics, nuclear chemistry and not least astrophysics. To understand what is going on in the inaccessible interior of a star we must make a model of the star which explains the known data: mass, diameter, luminosity, surface temperature and surface composition. The development of such a model normally starts with an assumption of how elemental composition varies with distance from the center. By solving the differential equations for pressure, mass, temperature, luminosity and nuclear reactions from the surface (where these parameters are known) to the star's center and adjusting the elemental composition model until zero mass and zero luminosity is obtained at the center one arrives at a model for the star's interior. The model developed then allows us to extrapolate the star's evolution backwards and forwards in time with some confidence. Figure 17.4 shows results from such modelling of the sun.

17.4.1. *Hydrogen burning to helium*

Helium can be formed from hydrogen in several ways, the least likely one is (17.5), which would require that 4 protons come together simultaneously. The possible multi-step processes are (not showing γ's)

$$^{1}H + {}^{1}H \rightarrow {}^{2}H + {*e^{-}} + e^{+}{*} + \nu_e \qquad Q = 0.42 + 1.02 = 1.44\ \text{MeV} \qquad (17.11)$$

$$^{1}H + {}^{2}H \rightarrow {}^{3}He \qquad Q = 5.49\ \text{MeV} \qquad (17.13)$$

$$^{1}H + {}^{3}H \rightarrow {}^{4}He \qquad Q = 19.81\ \text{MeV} \qquad (17.14)$$

$$^{2}H + n \rightarrow {}^{3}H \qquad Q = 6.25\ \text{MeV} \qquad (17.15)$$

$$^{2}H + {}^{2}H \rightarrow {}^{3}H\ (1.01) + {}^{1}H\ (3.02) \qquad Q = 4.03\ \text{MeV} \qquad (17.16a)$$

$$^{2}H + {}^{2}H \rightarrow {}^{3}He\ (0.82) + n\ (2.45) \qquad Q = 3.27\ \text{MeV} \qquad (17.16b)$$

$$^{2}H + {}^{2}H \rightarrow {}^{4}He \qquad Q = 23.85\ \text{MeV} \qquad (17.12)$$

$$^{2}H + {}^{3}H \rightarrow {}^{4}He\ (3.52) + n\ (14.06) \qquad Q = 17.58\ \text{MeV} \qquad (17.17)$$

$$^{2}H + {}^{3}He \rightarrow {}^{4}He\ (3.67) + {}^{1}H\ (14.67) \qquad Q = 18.35\ \text{MeV} \qquad (17.18)$$

TABLE 17.1. *The proton-proton chain for ^{4}He formation; about 90% of the solar energy production*

Reaction steps	Q (MeV)	Mean reaction time	
$^1H + {}^1H \rightarrow {}^2H + {}^*e^- + \beta^{+*} + \nu(2\%)$	1.44 MeV	1.4×10^{10} y	(17.11)
$^2H + {}^1H \rightarrow {}^3He + \gamma$	5.49 MeV	6 s	(17.13)
$^3He + {}^3He \rightarrow {}^4He + 2\,{}^1H$	12.86 MeV	9×10^5 y	(17.21)
Overall $4\,{}^1H \rightarrow {}^4He + {}^*2e^- + 2\beta^{+*} + 2\nu$	26.7 MeV	1.4×10^{10} y	(17.5)

$$^3H + {}^3H \rightarrow {}^4He\ (3.78) + 2n\ (7.55) \qquad Q = 11.33\ \text{MeV} \tag{17.19}$$

$$^3He + 2n \rightarrow {}^4He\ (4.27) + n\ (17.09) \qquad Q = 21.36\ \text{MeV} \tag{17.20}$$

$$^3He + {}^3He \rightarrow {}^4He\ (4.29) + 2\,{}^1H\ (8.57) \qquad Q = 12.86\ \text{MeV} \tag{17.21}$$

All reactions are exothermic. Figure 17.5 shows how reaction cross sections increase with temperature. As the number of particles of a particular energy decreases with energy (Fig. 17.3) this results in a maximum number of reactions at a certain energy, E_{max}. The fastest hydrogen fusion reaction is (17.17), which, however, requires that tritium has been synthesized in an earlier step, e.g. by (17.15) or (17.16a).

(i) For stars with $m \leq 1.5\ \mathbf{M}_\odot$ and $T \geq 2 \times 10^7$ K, the main reaction sequence is (17.11) followed by (17.13) and (17.21). This is referred to as the *proton-proton chain*, summarized in Table 17.1. Reaction times in Tables 17.1 and 17.2 are from Gamow and refer to solar conditions.

In 9% of the pp-chain, reaction (17.21) is replaced by

$$^3He + {}^4He \rightarrow {}^7Be \qquad Q = 1.59\ \text{MeV} \tag{17.22}$$

$$^7Be + e^- \rightarrow {}^7Li + \nu_e\ (4\%) \qquad Q = 1.37\ \text{MeV} \tag{17.23}$$

$$^7Li + {}^1H \rightarrow 2\,{}^4He \qquad Q = 17.34\ \text{MeV} \tag{17.24}$$

The neutrino takes 4% of the decay energy. To a very small amount ($<$ 1%) also the reaction sequence

$$^7Be + {}^1H \rightarrow {}^8B; \quad {}^8B + e^- \rightarrow {}^8Be \rightarrow 2\,{}^4He \qquad Q = 18.21\ \text{MeV} \tag{17.25}$$

occurs. Thus isotopes of Li, B and Be are formed as intermediates. ^{7}Be decays by electron capture (see Fig. 4.7) while ^{7}Li is stable. ^{8}B is very shortlived, decaying to ^{8}Be which immediately decays into 2 He. The number of p-p-fusion reactions in our sun amounts to $1.8 \times 10^{38}\ s^{-1}$. The solar neutrino emission comes to $\sim 15\%$ from reaction (17.23) (E_ν 0.38 – 0.86 MeV) and to $\sim 85\%$ from (17.11) ($E_\nu \leq 0.4$ MeV).

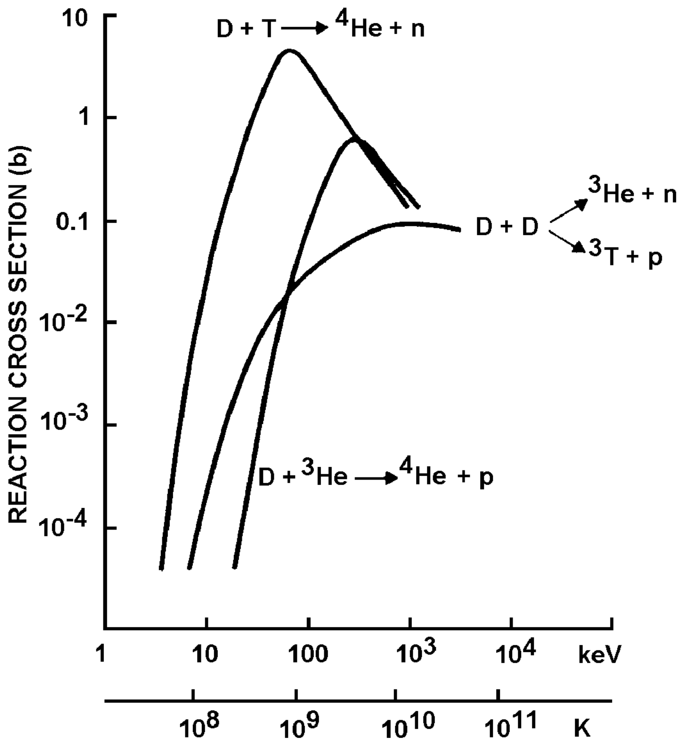

FIG. 17.5. Reaction cross sections for some light element fusion reactions at solar conditions. (From Bowler.)

(ii) For stars with $m \geq 1.4$ $\mathbf{M}_\odot$ Bethe and Weizsäcker in the 1930s deduced the so-called "*CNO-*" or *carbon cycle*, Table 17.2. In such stars temperature and pressure reach higher values, and the consumption of hydrogen is faster. A star of 20 $\mathbf{M}_\odot$ burns its hydrogen through the CNO-cycle in some 10 My, compared to the sun's pp-cycle, which burns hydrogen at a slower rate for about 10 000 My.

The CNO-cycle requires the presence of some ^{12}C, which acts as a catalyst. In a hydrogen burning star some small amounts of ^{12}C is always produced through reaction (17.30).

In our sun ~ 6% of the hydrogen originally in the core has now been burnt. Since helium has a greater mass than hydrogen, it accumulates in the core, while most of the hydrogen burning moves to a layer around the He. As the hydrogen fuel is consumed, the temperature of the core decreases somewhat. However, as the amount of helium is increased and the hydrogen depleted, the core contracts through the increased gravitational attraction of the helium, and the temperature of the core rises. This heats the outer layers of hydrogen and results in an expansion of the outer mantle of the star, which in turn results in a cooler surface, so that the star irradiates more red light. The star at this period of its life is referred to as a *Red Giant,* see Figure 17.1. We can expect that our sun in about five eons from now will pass through a red giant stage at which time its diameter should expand sufficiently to engulf the inner planets of the solar system.

TABLE 17.2. *The* CNO *cycle for helium production; about 10% of the solar energy*

Reaction steps	Q (MeV)	Mean reaction time	
$^{12}C + {}^{1}H \rightarrow {}^{13}N + \gamma$	1.94	10^{7} y	(17.26a)
$\downarrow$ $^{13}C + e^{-} + \beta^{+} + \nu$	1.20	7 min	(17.26b)
$^{13}C + {}^{1}H \rightarrow {}^{14}N + \gamma$	7.55	3×10^{6} y	(17.27)
$^{14}N + {}^{1}H \rightarrow {}^{15}O + \gamma$	7.29	3×10^{8} y	(17.28a)
$\downarrow$ $^{15}N + e^{-} + \beta^{+} + \nu$	1.74	2 min	(17.28b)
$^{15}N + {}^{1}H \rightarrow {}^{12}C + {}^{4}He$	4.86	10^{5} y	(17.29)
Overall $4\,{}^{1}H \rightarrow {}^{4}He + *2e^{-} + 2\beta^{+}* + 2\nu$	26.7	3×10^{8} y	(17.5)

17.4.2. *Helium-burning to iron*

(i) For stars with 0.26 $\mathbf{M}_{\odot} < m < 1.5\ \mathbf{M}_{\odot}$, the contracting helium core degenerates and warms. When a density of $\sim 10^{7}$ kg m^{-3}, and a temperature of $\sim 1.5\times10^{8}$ K are reached, He begins to fuse. Even though ^{8}Be has an extremely short lifetime, there is always a small equilibrium amount present. It has been calculated that in some red giants one ^{8}Be nucleus is in equilibrium with $\sim 10^{9}$ nuclei of ^{4}He. This amount is sufficient to allow some capture of a third helium nucleus to form ^{12}C. The reaction is

$$^{8}Be + {}^{4}He \rightarrow {}^{12}C \tag{17.30}$$

sometimes referred to as the "3α-process" as 3 He form a C atom. This produces a sudden heating at the center, and in fact the core can be considered to detonate, the *helium flash* (Fig. 17.1), though this detonation is dampened by the large outer masses. In such a star helium burning goes on in the core and hydrogen burning at the outer shell. As the central helium is exhausted, helium burning proceeds in an outer shell, while carbon collects in the center. For our sun the He-burning period is expected to last for only 60 My after which $\sim 50\%$ of the core will be C and O. The fusion reactions will then halt. The outer envelope, which through turbulent mixing includes some core material, expands and the star loses some of its mass. The expanding envelope forms a *planetary nebula* with the star in the center termed a white dwarf, see Figure 17.1.

(ii) Stars of masses $> 1.5\ \mathbf{M}_{\odot}$ burn hydrogen through the CNO cycle. This requires that the core be convective. The main sequence phase ends as the hydrogen in the core is exhausted, and shell burning begins. The helium core remains convective and nondegenerate, and helium burning begins without perturbations, leading to the formation of mainly carbon and oxygen.

(iia) Stars with 3 $\mathbf{M}_{\odot} < m < 15\ \mathbf{M}_{\odot}$ burn hydrogen and helium in outer shells. For stars of masses $> 3.5\ \mathbf{M}_{\odot}$ helium burning becomes the important energy source. Once ^{12}C has been formed, further reactions with helium can explain the formation of oxygen, neon and higher elements according to

$$^{12}C\ (^4He,\gamma)\ ^{16}O\ (^4He,\gamma)\ ^{20}Ne\ (^4He,\gamma)\ ^{24}Mg\ (^4He,\gamma)\ ^{28}Si \quad (17.31)$$

These reactions occur with increasing yields in stars of increasing mass.

(iib) Carbon fusion can occur in stars $> 7.5\ \mathbf{M}_\odot$ and at core temperatures $\geq 8\times10^8$K:

$$\begin{aligned} ^{12}C + {}^{12}C &\rightarrow {}^{24}Mg \\ &\rightarrow {}^{23}Na + {}^{1}H \\ &\rightarrow {}^{20}Ne + {}^{4}He \end{aligned} \quad (17.32)$$

This occurs suddenly, and is observed as a *carbon flash*, Figure 17.1. The star then either continues to burn carbon, or explodes (a *supernova*) with destruction of most of the star.

(iic) In the very heavy stars, $m > 15\ \mathbf{M}_\odot$, the He-burning only lasts for a few My. The carbon core formed remains convective, and carbon burns to oxygen and magnesium. Further fusion synthesis occurs in several zones, leading to the production of elements up to ^{40}Ca, ^{44}Ti, ^{48}Cr, ^{52}Fe and ^{56}Ni, partly by He-capture partly by direct fusion of heavier nuclides. The heaviest elements may be formed in reactions like

$$^{28}Si + {}^{28}Si \rightarrow {}^{56}Ni\ (\beta^+,\ 6.1\ d)\ {}^{56}Co(\beta^+,\ 77.3\ d)\ {}^{56}Fe\ (stable) \quad (17.33)$$

From Figure 3.3 it is seen that formation of elements higher than those of *A* around 60 through fusion processes are exoergic (i.e. requires energy). When fusion processes end the star consists of an iron core surrounded by shells with silicon, oxygen, carbon, helium and hydrogen. Material is continually lost to space, propelled by strong solar winds. Massive stars of 20 $\mathbf{M}_\odot$ lose as much as 1/100 000 of their mass every year. The outer layer may have a temperature of only a few million degrees, while the center may be 10^9 K. In the lover density outer layer we might expect to find Li, Be, and B. However, these elements have been consumed in reactions with lighter nuclides.

The last steps of production of heavy elements (up to Fe/Ni) occurs rather rapidly in a few thousand years. When the nuclear fuel for fusion is exhausted the star collapses and results in a *supernova*. Figure 17.6 illustrates the composition of a 20 $\mathbf{M}_\odot$ star just before a supernova explosion.

The sequence of element formation is summarized in Figure 17.7a (from the famous paper by Burbidge, Burbidge, Fowler and Hoyle). Figure 17.7b is from same paper and shows the calculated elemental composition, which is not too different from that in Figure 17.2a.

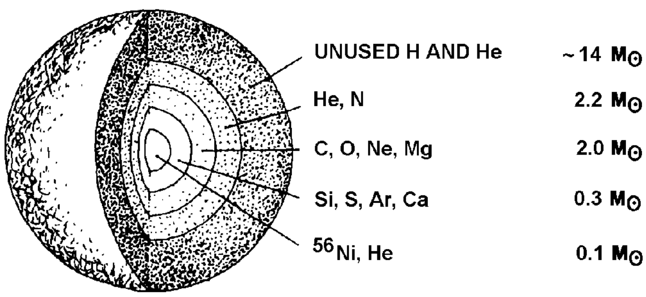

FIG. 17.6. Shell structure of a 20 $M_\odot$ star just before supernova explosion.

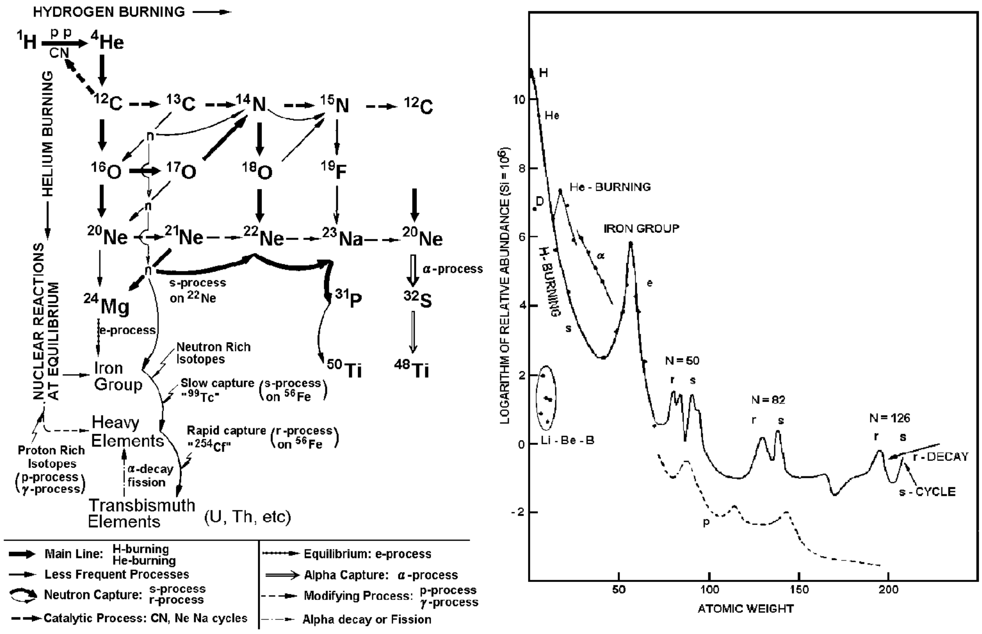

FIG. 17.7. a. Schematic diagram of the nuclear processes for synthesis of the elements in stars.
b. Calculated atomic abundances. (From Burbidge, Burbidge, Fowler and Hoyle.)

The short half-life of ^{8}Be plays a significant role. If ^{8}Be was much more stable, the helium-consuming chain would have proceeded much more rapidly. In fact after the helium ignition the energy production rate would have increased enormously and the red giant would have exploded as a supernova. However, the burning would not have gone much further than to ^{12}C. On the other hand, was ^{8}Be less stable, the fusion synthesis would never have been able to bridge the mass 8, and no elements higher than Be would have been formed.

The Q-value for the reaction $^4\mathrm{He} + {}^{12}\mathrm{C} \rightarrow {}^{16}\mathrm{O}$ is 7.16 MeV. The excited levels of ^{16}O near this value are 7.12 and 8.87 MeV. The 8.87 MeV level is not useful for ^{16}O production since the Boltzmann distribution provides too small a fraction of particles with the needed kinetic energy. However, the resonance width of the 7.12 MeV level makes the reaction possible for the high energy tail of the Boltzmann distribution. Had it been easier to make ^{16}O, we would have had less carbon and more oxygen in the universe. This probably would have been a hindrance in the development of life, since it is believed that life must start in a reducing (low oxygen containing) atmosphere.

Our galaxy has stars much larger and much smaller than our sun, and of widely different ages. Thus the processes we have described are occurring at present in the Milky Way and in other galaxies as well. Moreover, the stars emit considerable amounts of matter into space. As a result, interstellar gas, out of which new stars are formed, contains atoms heavier than helium, although hydrogen is the most abundant element.

17.5. Neutron capture processes: from iron to uranium

Figure 3.3 shows that the maximum nucleon binding energy occurs at $A \approx 60$, i.e. around iron, which we may consider to be the most thermodynamically stable element in the universe. At lower values of A, fusion of lighter elements releases energy while the exothermic reactions to form heavier elements ($A > 60$) involve neutron capture.

17.5.1. *Slow neutron capture*

Through hydrogen and helium burning, neutrons are formed. The most important reaction is believed to be

$$^{22}\mathrm{Ne} + {}^{4}\mathrm{He} \rightarrow {}^{25}\mathrm{Mg} + \mathrm{n} \tag{17.34}$$

As the heavier elements form in the star, the neutron production increases considerably since such reactions become more prevalent as heavier elements are involved in the reactions. In reactions like (17.32) and (17.33) energetic γ-rays are emitted, which decompose D into H and n (the binding energy is 2.22 MeV). The mode of production of the elements changes from that of helium capture to that of neutron capture, so that the elements from iron to bismuth can be formed by a slow process of neutron capture (n,γ-reactions), interrupted by β-decay whenever it is faster than the next capture step.

Such a process is known as the *slow*, or *s-process*. While the reaction probability for the capture of neutrons increases with the atomic number of the element, the relative amount of the elements in the star will decrease with increasing atomic number, because of the successive higher order of reaction (§15.3). The result is the observed flattening of the abundance curve for $A > 100$, see Figures 17.2a and 17.7b.

The formation of ^{104}Pd from ^{100}Ru can serve as an example of the steps in the s-process of element formation

$$
\begin{array}{lll}
{}^{100}_{44}\mathrm{Ru}\ (\mathrm{n},\gamma)\ {}^{101}_{44}\mathrm{Ru}\ (\mathrm{n},\gamma)\ {}^{102}_{44}\mathrm{Ru}\ (\mathrm{n},\gamma)\ {}^{103}_{44}\mathrm{Ru} & & \\
\qquad\qquad\qquad\qquad\qquad\qquad\quad \beta \downarrow 39\ \mathrm{d} & & \\
\qquad\qquad\qquad\qquad\qquad\qquad\quad {}^{103}_{45}\mathrm{Rh}\ (\mathrm{n},\gamma)\ {}^{104}_{45}\mathrm{Rh} & & \\
\qquad\qquad\qquad\qquad\qquad\qquad\quad (\mathrm{stable}) \qquad \beta \downarrow 42\ \mathrm{s} & & \\
\qquad\qquad\qquad\qquad\qquad\qquad\qquad\qquad {}^{104}_{46}\mathrm{Pd}\ (\mathrm{stable}) & &
\end{array} \tag{17.35}
$$

Note that ^{100}Ru to ^{102}Ru are stable.

The discovery of the element promethium (for which the longest-lived isotope has a half-life or only 18 y) in a star (HR 465) in the Andromeda constellation shows that an s-process must be occurring. A possible reaction path is

$$^{146}\mathrm{Nd}\ (\mathrm{n},\gamma)\ {}^{147}\mathrm{Nd}\ (\beta^-,\ 11\mathrm{d})\ {}^{147}\mathrm{Pm}\ (\beta^-,\ 2.6\ \mathrm{y}) \tag{17.36}$$

The s-process is believed to be extensive in Red Giant stars of mass 3 – 8 $\mathbf{M}_\odot$ and to last for about 10 My, a short period in the total lifetime of a star.

As the star proceeds through the s-process stage we can expect that the fusion reactions decrease while the gravitational contraction of the star continues. To conserve angular momentum the rotational velocity increases, resulting in the ejection of some of the outer mantle into space, thereby exposing the inner, hotter core. Thus in the radio source Cassiopeia A one can see fast moving "knots" of O, S and Ar. The turbulence is likely to bring up heavier elements from the core, as observed in the CP-stars (§17.1.6). For example, the light from the planetary nebula nucleus of FG Sagittae suddenly showed strong barium lines between 1967 and 1972. The turbulence may become so violent that hydrogen from outer layers is mixed in with deeper layers of higher temperature, leading to instantaneous hydrogen burning and a very rapid rise in energy production. This is observed as a sudden light increase from the star (*nova*). After the nova stage (or stages, as several such may occur) the star would continue to cool until it becomes a white dwarf. The density of such a body would be very large, about 10^8 kg m^{-3}.

17.5.2. *Supernova explosions*

The s-process cannot explain the formation of the elements heavier than bismuth as the trans-bismuth elements have a number of short-lived isotopes which prevent the formation of thorium and uranium in the amounts observed in nature. The heaviest elements are believed to be formed in supernova explosions.

In a star in which heavier elements are accumulated in its center, the energy production occurs in the layer surrounding the core, see Figure 17.6. For stars of an original mass > 7.5 $\mathbf{M}_\odot$ (or > 3.5 $\mathbf{M}_\odot$ at the end of the helium-burning period) the energy loss through photon and, especially, through neutrino emission is very large. This has several consequences:

(i) the emission of energy into space cools the core and the giant begins to contract,

(ii) the atoms in the core can no longer resist the tremendous pressure and their electron shells collapse (forming degenerate matter),

(iii) the contraction and pressure in the core increase to nuclear density (ca. 10^{17} kg/m^3), and the released gravitational energy increases temperature and pressure also in the outer layers.

Under the development of these conditions, the elements in the core disintegrate (especially iron) releasing helium and neutrons; e.g.

$$^{56}\mathrm{Fe} + \gamma \rightarrow 13\,^{4}\mathrm{He} + 4\mathrm{n} \qquad (17.37)$$

The helium immediately fuses and the intense heat developed spreads as a heat shock, which passes to the cooler outer shells of hydrogen and helium, initiating new thermonuclear reactions in the mantle. As a result the whole star explodes as a supernova. While the outer layers expand into space, the core contracts to a *black hole*. Other mechanisms producing supernovae are also known.

A supernovae can be seen by the naked eye as a new star if it occurs within our galaxy. The light intensity slowly decreases and the star may be too weak to see after a year. A supernova discovered by Kepler in 1604 could be seen even in day time and its expanding gas cloud is still easily observed by telescope. The next "nearby" supernova (SN1987A) was seen, on February 24, 1987, in the Large Magellanic Cloud. Before the light arrived to us, a high energy (20 – 40 MeV) neutrino emission (a total of 19 electron anti-neutrinos was measured in 10 s, compared to a normal 2 per day) was observed in Japanese and American detectors (cf. §10.6), proving that a large neutrino burst ($\sim 10^{58}$ neutrinos) accompanied the supernova explosion. The neutrinos had an energy corresponding to 5×10^{10} K, and the total gravitational energy released in the process was estimated to 3×10^{46} J.

SN1987A was of a composition like that in Figure 17.6. At the high temperature of the explosion, most of the lighter atoms fused into Fe/Ni, which, thus is not only consumed but also produced "further out". The ^{56}Ni decays according to

$$^{56}\text{Ni (EC, 6.1 d)}\ ^{56}\text{Co (EC, 77.3 d)}\ ^{56}\text{Fe (stable: 91.7\%)} \qquad (17.38)$$

The light from the supernova could be related to 0.85 and 1.24 MeV γ-lines from the decay of ^{56}Co; Figure 17.8 shows the decay curve. One could actually calculate that in the first moments after the explosion about 0.1 $\mathbf{M}_\odot$ of ^{56}Ni was formed. Most of the Fe in the Universe is likely produced by this kind of process.

The mass of heavy elements spewed out into space enriches it for the formation of later generation stars. The transition elements, which are only formed in such stellar explosions, are a necessity for the existence of life on earth.

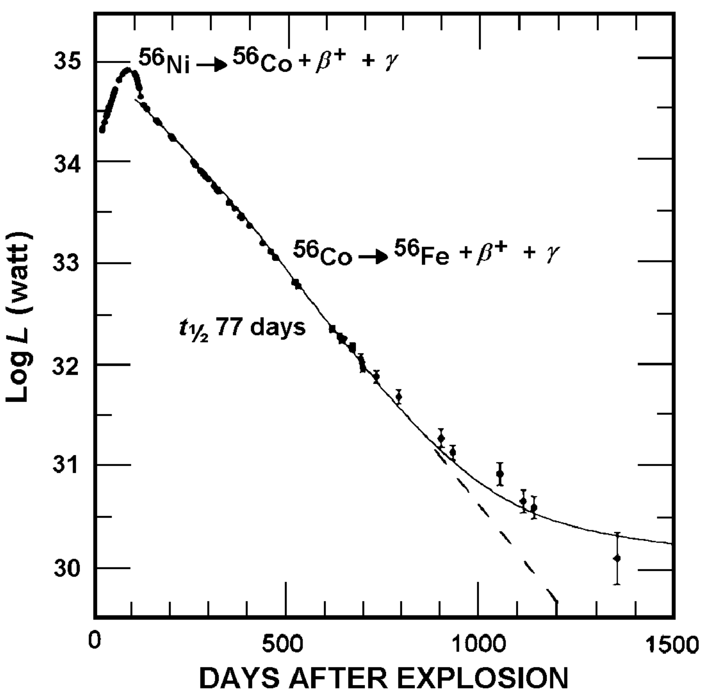

FIG. 17.8. Luminosity of SN1987A as function of time. (From Fransson.)

17.5.3. *The rapid (r-) process*

The supernova stage is very short-lived with extremely intense neutron production. It provides a method whereby the barrier of the short-lived isotopes between polonium and francium is overcome and the heaviest elements synthesized. This mode of element formation is known as the *rapid* or *r-process*; see Figure 17.9.

The n-capture in the r-process has been suggested to go up to Z about 100 and $N \leq 184$. In the intense neutron field a considerable amount of (mainly fast) fission of the newly synthesized heavy elements probably also occurs. This partly explains the peaks at $N = 50$ and 82 in Figure 17.7b, which also correspond to maximum yields at $A = 95$ and 140 in thermal fission. Some stars are unique in that they have an unusually high abundance of fission products; spectral lines from heavy actinides, like americium and curium, have also been observed in such stars.

The explosion of thermonuclear hydrogen bombs containing uranium resulted in the formation of elements 99 and 100 (§16.2.5). These elements were synthesized in the extremely short time of the explosion by the intense neutron flux bombarding the uranium (shaded area in Figure 16.4). The explosion of the hydrogen bomb duplicated in a very small way what is believed to be the process of the formation of the heaviest elements in supernovae. The neutron fluxes and exposures in the s- and r-processes as compared to those in a nuclear explosion and a reactor are given in Table 17.3.

The intensity of the neutron flux as well as the very short time preclude β-decay as a competitor to neutron capture in the r-process. This results in a different isotopic distribution of the elements for the r-process compared to that formed in the s-process. The following reaction sequence illustrates the r-process in which β-decay can occur only after the explosion has terminated and the intense neutron fluxes decreased (compare with the sequence (17.35)):

$$\begin{array}{ccccccc}
{}^{100}\mathrm{Ru}\ (n,\gamma)\ {}^{101}\mathrm{Ru}\ (n,\gamma)\ {}^{102}\mathrm{Ru}\ (n,\gamma) & {}^{103}\mathrm{Ru} & (n,\gamma)\ {}^{104}\mathrm{Ru}\ (n,\gamma) & {}^{105}\mathrm{Ru} & (n,\gamma) & {}^{106}\mathrm{Ru} \\
& \beta\downarrow 39\ \mathrm{d} & & \beta\downarrow 4.4\ \mathrm{h} & & \beta\downarrow 368\ \mathrm{d} \\
& {}^{103}\mathrm{Rh} & & {}^{105}\mathrm{Rh} & & {}^{106}\mathrm{Rh} \\
& \text{(stable)} & & & & \\
& & & \beta\downarrow 36\ \mathrm{h} & & \beta\downarrow 30\ \mathrm{s} \\
& & & {}^{105}\mathrm{Pd} & & {}^{106}\mathrm{Pd} \\
& & & \text{(stable)} & & \text{(stable)}
\end{array} \qquad (17.39)$$

TABLE 17.3. *Comparison of conditions for n-capture processes*

Process	Flux (n m^{-2} s^{-1}) x	time =	exposure (n m^{-2})
s-process	$\sim 10^{18}$	$\sim$ 1000 y	$\sim 3 \times 10^{29}$
r-process	$> 10^{29}$	1–100 s	$> 10^{29}$
nuclear explosion	$> 10^{33}$	$<$ 1 μs	$\sim 10^{27}$
nuclear reactor	$\sim 10^{16}$	$\sim$ 1 y	$\sim 10^{23}$

After completion of the r-process, ^{103}Ru, ^{105}Ru, ^{106}Ru undergo β-decay to isotopes of Rh and Pd. In this r-sequence ^{104}Ru – ^{106}Ru are formed, but in the s-sequence beginning with ^{100}Ru, the heaviest ruthenium isotope has $A = 103$.

In the supernova explosion a large mass of material is ejected into interstellar space. This contributes to the higher abundance of heavy elements in cosmic rays as compared with the cosmic abundance. In fact, even uranium has been observed in cosmic rays and in our sun. Since our sun is undergoing the simplest type of hydrogen-burning cycle, it is not possible for the heavier elements ($\sim 2\%$) to have been synthesized by the sun. Consequently, their presence indicates that the sun has been formed as a second (or later) generation star from material that included matter ejected by an earlier supernova, or has accumulated matter from such a star.

The carbon cycle stars are likely to be second generation stars because ^{12}C is needed in the core for the carbon cycle to start. The same star may pass through several novae explosions whereby it loses large amounts of the lighter elements from the outer mantle in each explosion. The chemical composition of a star thus not only indicates its age but also tells us to which generation of stars it belongs.

17.5.4. *Neutron stars*

A supernova explosion leaves a residue at the center of the expanding gas cloud generated by the explosion. This residue is believed to contract into a neutron star. Assuming a nucleon radius of 0.85 fm, the density becomes about 2×10^{18} (cf. also Figure 3.4 for densities of other nuclear matter). When the central (remaining) mass of the supernova has contracted to a density of $> 10^{17}$ kg m^{-3} matter will consist of relatively closely packed nuclei and free electrons. It now becomes favorable for the protons to capture electrons

$$p + e^- \rightarrow n + \nu \tag{17.40}$$

The neutrinos are emitted and only neutrons are left.

The neutron star has a considerable energy reservoir in its rotation, typically one rotation per second. Particles ejected from this rapidly rotating object would be caught in the rotating magnetic field and accelerated to relativistic tangential velocities. They emit high intensity bremsstrahlung, which appear as pulses of radiation with the frequency of the rotation. Such radiation pulses have been observed from cosmic sources known as *pulsars*. The discovery of a pulsar at the center of the expanding Crab nebula, which is the remnants of a supernova explosion observed by the Chinese in the year 1054 has provided strong evidence for the model outlined above. Pulsars have been suggested to be the source of the high energy cosmic ray particles observed in our atmosphere.

17.6. Age of the Galaxy

Estimates of the age of our galaxy comes mainly from theoretical calculations. However, radiochemical investigations can yield information about several important steps. Thus the time since the final solidification of the earth's crust is obtained from the dating of geologic samples (Ch. 5). Nuclear clocks like U → Pb give only the age of minerals; the oldest known minerals on earth are 3.7×10^9 y.

Some glassy materials in meteorites and from the moon are assumed to be original condensed matter which never has undergone melting. The oldest ages seem all to converge at 4.6×10^9 y. Thus we conclude that this was the time when our planetary system began to form (the basis for the estimate of the age of our sun in §17.1.4).

Further information about this event has been obtained by studying tracks which nuclear decay processes leave in certain minerals (§8.1.2). Fission tracks can only persist in minerals that have not been heated because heating above 600°C erases the tracks. The fact that ^{244}Pu fission tracks have been found in iron meteorites and in lunar samples shows that ^{244}Pu existed when the planetary system formed. Because of the short half-life of ^{244}Pu (8×10^7 y) it can be concluded that such mineral samples must have formed within a few hundred million years after the nuclide ^{244}Pu itself was formed. This is probably also the time for planetary formation. The existence of primordial plutonium indicates that an r-process preceeded the formation of the planets.

Apparently, our solar system was showered by debris from a recent but distant supernova explosion which may have disturbed the "peaceful" gas cloud in our part of the universe and initiated the condensation of the solar system. At this time newly formed elements stopped being added to the solar system from the galaxy. Sufficient amounts of ^{129}I and ^{244}Pu remained after the formation of solid materials to produce characteristic isotope anomalies and fission track excesses in meteoritic and lunar materials. The spontaneous fission decay of ^{244}Pu yields ^{129}I, which decays as

$$^{129}\mathrm{I} \xrightarrow[1.6 \times 10^7 \mathrm{~y}]{\beta^-} {}^{129}\mathrm{Xe} \text{ (stable)} \tag{17.41}$$

The fact that meteorites containing about 100 times excess fission tracks also contain ^{129}Xe is evidence both for the existence of ^{244}Pu at the beginning of the collapse of the solar nebula, and for the rapid condensation of the meteorites from freshly produced new elements. This time has been calculated to about 80 My from the isotopic concentrations. By similar analysis we can go further back in the history of the universe and calculate the time between the formation of the elements in the galaxy and the condensation of the solar system; the result yields a time of 9.9×10^9 y (or 9.9 eons).

Recently there has come new radiochemical evidence about the age of our Galaxy. Consider Figure 17.9, which shows a part of a nuclide chart; the zigzag arrow shows nuclides formed in the s-process, the lower right arrows nuclides formed by the r-process. ^{186}Os can only form in the s-process and ^{187}Re only in the r-process. It is likely that our solar system, and ^{187}Re, was formed from a supernova in the r-process. ^{187}Re decays ($t_{1/2}$ 46×10^9 y) to ^{187}Os, which also is formed from slow n-capture in ^{186}Os. The amount of ^{187}Os formed in the s-process can be calculated from estimated flux values and known cross sections (at 30 keV; 3.6×10^8 K). Thus the amount of ^{187}Os formed by decay of ^{187}Re can be calculated, and the time since the r-process determined. This rhenium-osmium clock gives us an age of 10.8 ± 2.2 eons from formation of the Galaxy until our solar system formed. If this is combined with the age of the solar system of 4.7 eons, the age of the galaxy becomes 15.5 ± 2.3 eons. Adding 1.5 eons for the time between the Big Bang and the formation of the Galaxy, the universe should have an age of 17 ± 3 eons.

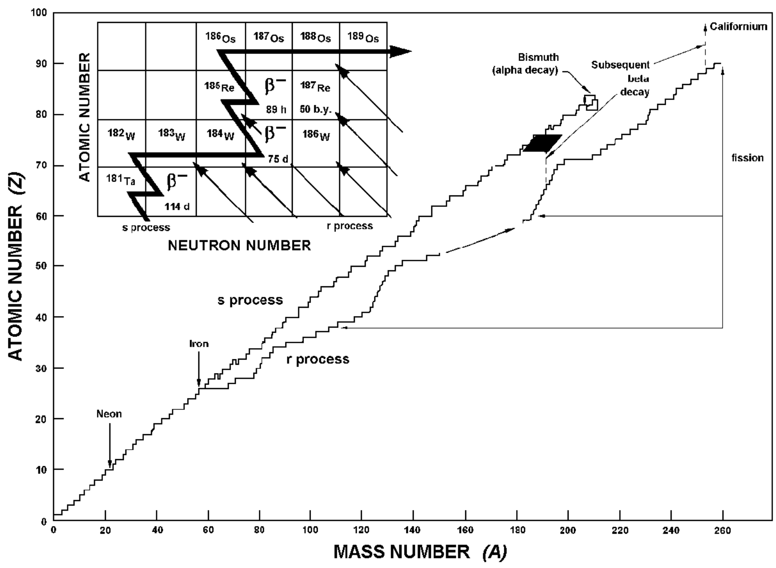

FIG. 17.9. Part of isotope chart showing the formation of W, Re and Os isotopes by the s- and the r-processes.

This value should be compared with the most recent value of t_0 (17.4b), which without a correction for any change in the rate of expansion, gives 16.6 ± 1.7 eons. With correction for deceleration the age should be significantly less than 16 eons. The agreement between the uncorrected value, 16.6 eons, and the value, 17 ± 3 eons, above indicates either that the Universe continues to expand at an unchanged rate, or if it does not, that

(i) Hubble's law is not valid, or
(ii) the cosmological (Einstein) constant is not unity, or
(iii) something is wrong with the Big Bang hypothesis, or
(iv) the radiometric data are too uncertain, or
(v) the expansion of the universe accelerates slowly (as indicated by resent measurements).

17.7. The evolution of the planets and the Earth

The planets are assumed to have formed out of the same cloud as, and simultaneously with, the sun. The sun contains 99.85% of the mass of the solar system, the planet Jupiter 0.1%, and all other planets 0.04%. The originally spherical cloud was disturbed and caused to rotate through some external action (e.g. supernova explosion or passage of some celestial body), the rotation leading to the formation of a disk-like cloud, and later to cloudy rings similar to those one can see around many stars and some of the planets. The cloud condensed successively into dust particles, which through collisions formed larger particles until rather large clumps of sizes similar to the present asteroids were obtained (so-called *planetesimals*, with diameters of several km; compare the sizes of the craters on the moon). By the time these clumps drifted together (a process referred to as *accretion*) to form the protoplanets, which collected more dust and gas from the surrounding cloud. When the

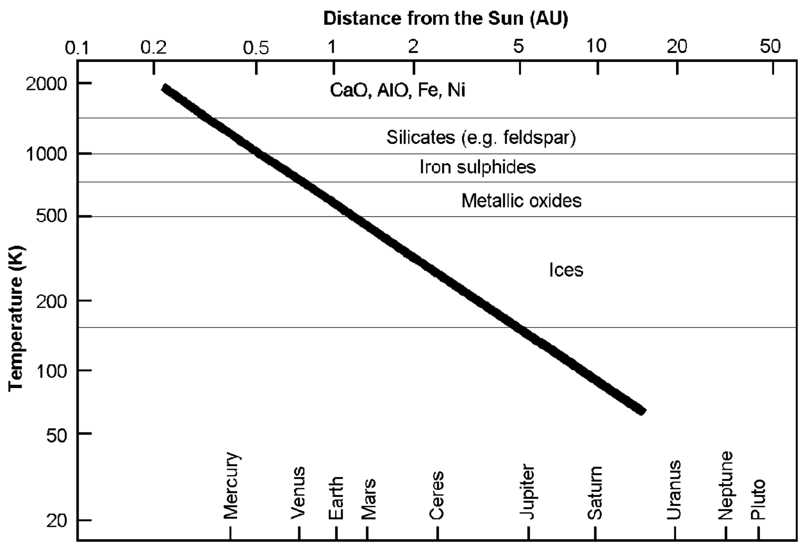

FIG. 17.10. Temperature distribution in the solar system during planet formation. (From Karttunen et al.)

H-burning started in the sun, a strong solar wind was produced, which blew away the gas and dust left in the cloud, and the planet formation was in principle finished. Some cosmogonists think this whole process took place in only a few million years.

The temperature gradient in the primordial elliptical cloud is given in Figure 17.10 with condensation temperatures for important elements and compounds. The volatile elements are almost completely absent in the innermost ("terrestrial") planets (Mercury, Venus, Earth, Mars). Here rock-forming minerals were produced in high-temperature chemical processes (Al_2O_3, SiO_2, $CaTiO_4$, $Ca_2Al_2SiO_7$, etc) and condensed out together with little volatile metals (Fe, Ni, etc). At lower temperatures further out in the solar system, H_2O was formed and condensed out as ice; e.g. some moons of Saturn are almost pure ice. At still lower temperatures NH_3 and CH_4 would liquefy. Jupiter and Saturn contain 99% H_2, 0.1% He, the rest being mainly H_2O (ice), CH_4 and NH_3; wide storms of NH_3-crystals have been observed on Saturn; Pluto has a thin atmosphere of only CH_4. Owing to the high pressures and low temperatures at these giant planets, hydrogen is either in the liquid or solid (metallic) state.

From assumptions of the elemental composition and temperature-pressure conditions of the solar system one can in principle calculate the average mineral composition of the Earth using thermodynamic data of known compounds. Several such calculations have been made, which more or less well account for the present composition of the crust, magma, etc. There are, however, some other observations which need comments.

According to Urey, Suess, and others, the accretion of cosmic particles during the formation process released gravitational energy; also the higher concentration of radioactive nuclides in the primordial cloud (Fig. 17.11) contributed to heat and melt the solid material of our Earth-to-be. The Earth's temperature was 40 – 50% higher than today about 3.3 Gy ago. Not until a solid crust was formed could the radioactive clock begin to tick. This did

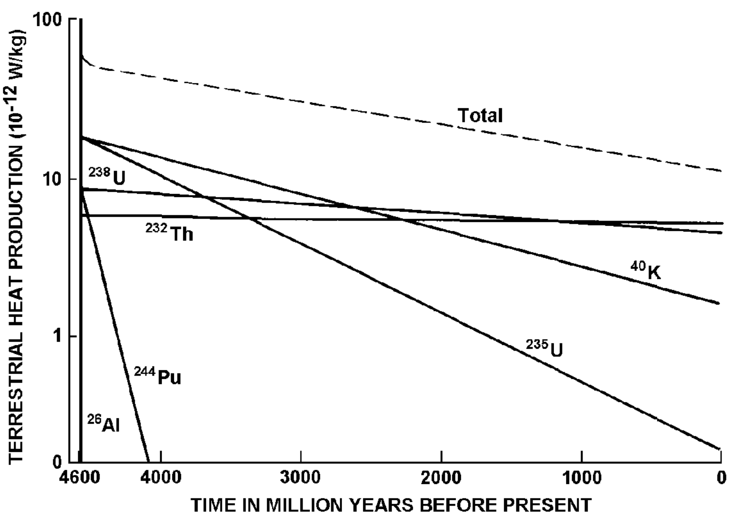

FIG. 17.11. Heat production from decay of radioactive species in earth. (From Brown and Musset, acc. to Cox.)

not occur until about 3.7 eons ago, as this is the age of the oldest minerals found on Earth. Thus, it should have taken about 1 eon for the Earth to solidify. As soon as the temperature fell below 100°C water could begin to condense, possibly leading to an abrupt global temperature reduction, due to cloud formation and high heat of vaporization.

All planets were originally formed with some atmosphere, partly as a remnant of the primordial cloud, partly due to outgassing of the interior through volcanos and to impacts of comets. The atoms/molecules in the atmosphere have an average velocity, which must be less than the escape velocity from the planet if the gases should not evaporate into space. The escape velocity depends of temperature and mass of the planet (cf. §17.1.2); for example, the moon has too small a mass to keep any atmosphere. The escape velocity of H_2 and He from the Earth is too large for these elements to be retained. The original atmosphere of the Earth is therefore believed to have been mainly H_2O, CO_2, N_2, CH_4 and NH_3. This is referred to as a *reducing atmosphere*, which probably is typical for all new-born Earth-sized planets. The UV-radiation from the sun decomposes these molecules (though the fragments may recombine), releasing H_2, which escapes. The O_2 released is very reactive and combines with many elements to form oxides; most of the red surface of Mars is FeO. The common assumption is that very little oxygen was originally present as free O_2. However, rather rapidly, processes led to a shift of the atmosphere from reducing towards *oxidizing conditions*. Life appears to have begun before this transition as evidenced by fossile bacteria-like organisms in very old rocks formed in a reducing atmosphere.

17.8. Controlled thermonuclear reactions

From earliest times man has become increasingly dependent of a variety of energy sources: heat from burning of wood, animal dung, coal, oil, natural gas, etc., mechanical energy from steam engines, wind mills and water falls, and electricity from the same sources as well as from nuclear reactors. Much effort has been invested in searches for new energy sources, preferably of the "renewable" kind in contrast to the non-renewable sources[1]. Energy is a strategic resource, playing an important role in international and national politics.

For more than 50 years scientists have studied methods of copying the fusion energy processes occurring in the sun in which hydrogen is transformed into helium. The availability of hydrogen and deuterium in the sea is so large that it will outlast any other non-renewable energy sources for any population growth rates: 1 liter of sea water contains deuterium with an energy content equivalent to 300 liter of gasoline (reaction 17.12).

At the first Geneva conference on the peaceful uses of atomic energy in 1955 there was strong sentiment that controlled thermonuclear reactors (CTR) would be in operation within 15 years. The optimism has gradually vanished as research has uncovered numerous technical difficulties. At present, it seems quite unlikely that such reactors will be in operation before the year 2050, although extensive research is being conducted towards CTR's, and great progress is being made. The following sections briefly describe the principal concepts, and some of the problems of controlled thermonuclear (fusion) power generation.

17.8.1. *The controlled thermonuclear reactor* (*CTR*)

Fusion reactions are most easily achieved with hydrogen atoms because of the low coulomb barrier and favorable wave mechanical transmission factor. The threshold reaction energy (E_{CB}(min), eqn. (12.14)) for the $^1H + {}^1H$ reaction is 1.11 MeV, which corresponds to an average temperature of 10^{10} K; at 10^8 K the fraction of particles with an energy $\geq$ 1.11 MeV is about 10^{-55}, at 10^9 K about 10^{-5}, and at 10^{10} K about 0.5. The quantum mechanical tunnel effect allows the reaction to proceed at an acceptable rate at lower temperatures: For the D + T reaction the ignition temperature is 3×10^7 K and for the D + D and D + ^{3}He reactions it is 3×10^8 K. These reactions are the prime candidates for controlled fusion; see Figure 17.5. Of the number of designs proposed for CTR's the present discussion is limited to inertial confinement and magnetic confinement systems.

17.8.2. *Inertial confinement*

Inertial confinement is a pulsed operation system. Small pellets of solid D_2 and T_2 ($\leq$1 mm) are placed into the middle of a chamber where the pellets are irradiated by intense beams of photons (from lasers) or electrons (from accelerators). The surface of the pellet rapidly vaporizes, resulting in a jet-stream of particles away from the pellet and an impulse (temperature-pressure wave) which travels into the pellet, increasing the central temperature to $> 10^8$ K. This causes a small fusion explosion, producing energetic ^{4}He and n (17.17). Because the particle density is high, the pulse time can be very short and still meet the

1 In a wider context, all energy originates from gravitational collapse, annihilation, fusion reactions or mass loss into black holes and its sources are thus never renewable.

Lawson criterion (see below). Temperatures of $\sim 10^9$ K have been reached with electron beams, and fusion neutrons produced. With a repetition rate of ~ 100 pellets s^{-1}, a power output of 1 – 10 GW would be achieved. Difficulties which have hampered the development include problems of shielding against the 14 MeV neutrons and of extraction of the released kinetic energy.

17.8.3. *The magnetic confinement reactor*

At $T = 10^7$ K, hydrogen atoms are completely dissociated into H^+ and free e^- (the plasma state). Because no construction material can withstand a plasma of this energy, it is necessary to keep it away from walls, which can be done by using strong magnetic fields, which is the same principle as used in mass spectrometers or cyclotrons. Of the various designs of "magnetic bottles", the torus (Fig. 17.12) seems to be the most promising and is the design chosen for further development in several national and international programs. The first torus machine was built in Moscow and named Tokamak; these machines have since then been called *tokamaks*.

Several factors determine the possibility of achieving a thermonuclear fusion reaction: the particle energy, which is related to the temperature (§2.6.2), the particle density and the reaction rate. These are connected in three design criteria:

(i) the *fusion reaction rate* parameter σv, where σ is the reaction cross section (which depends on the particle energy, cf. Fig. 17.5), and v the relative speed, or temperature, of the ions, averaged over the Maxwellian velocity distribution (the temperature must be $\geq 10^8$ K),

(ii) the *Lawson limit* $n\tau$, where n is the particle density and τ the confinement time, which indicates the ability of the plasma to retain its heat and is also called the *confinement quality* — the product must be $\geq 10^{20}$ particles s m^{-3} for the DT-reaction, and $\geq 10^{21}$ s m^{-3} for the DD-reaction,

(iii) the *fusion product* $n\tau T$, where T is the average ion temperature; this product must be $\geq 5 \times 10^4$ s eV m^{-3}.

The steady state reactor is limited in power density by heat transfer and other considerations to about $n = 10^{20} - 10^{21}$. Since each collision involves two particles, the fusion power density varies as the square of the particle density. At 1 Pa (i.e. 3×10^{20} particles m^{-3}) the power density would be tens of MW per m^3. This leads to a required confinement time of about 0.1 – 1 s.

Several large machines based on magnetic confinement have been built. The best results so far obtained, though not simultaneously, are: central ion temperature of 35 keV (4×10^8 K), confinement time of ~ 2 s, particle density of $\sim 5 \times 10^{19}$. Figure 17.13 shows the results obtained with different machines. Table 17.4 lists the results obtained with the JET machine and design parameters for ITER (International Thermonuclear Reactor Experiment). JET (Joint European Torus), the largest tokamak machine in operation, is an international project located at Abingdon, England. ITER is also an international experimental project which is expected to produce > 1000 times the power of JET. If promising results are obtained with ITER, it is planned to be followed by a power prototype, possibly some time after 2030 A.D.

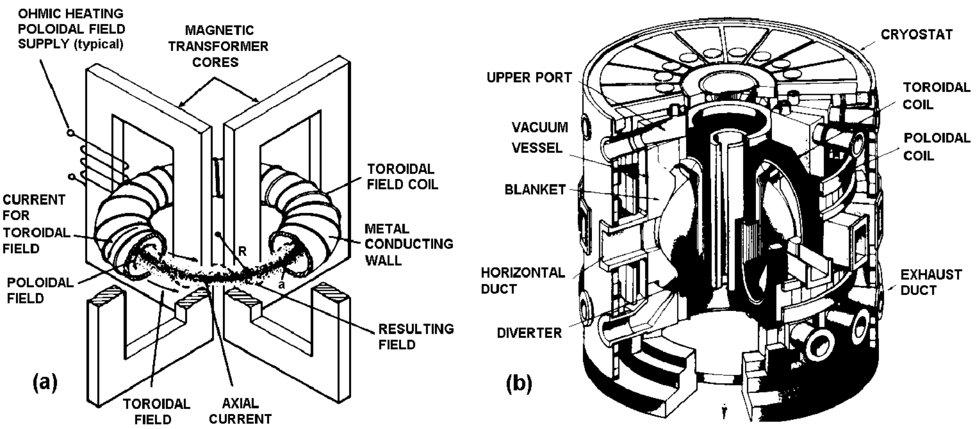

FIG. 17.12. (a) The torus magnetic confinement principle. (b) Schematics of the JET (or ITER) tokamak experimental reactor.

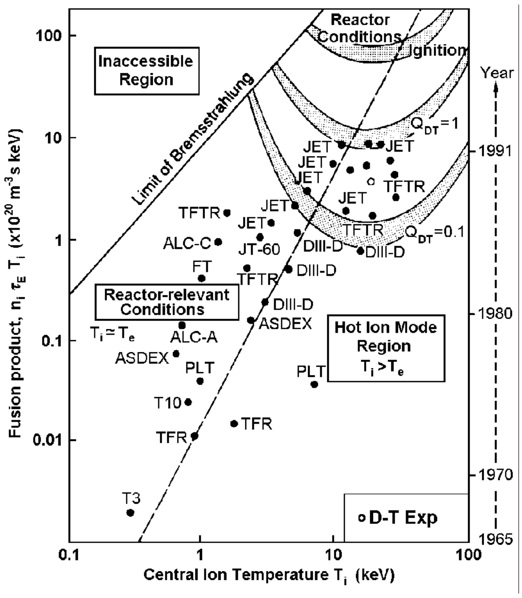

FIG. 17.13. Results obtained by different fusion reactor designs.

17.8.4. *Technical issues of a large CTR*

(a) *Particle injection and withdrawal*. In a steady state machine, whether it operates in pulsed mode or not, fuel (i.e. D and T) must be injected and, after consumption, reaction products (^{3}He, ^{4}He) must be withdrawn. Because of the strong magnetic field, injection of

TABLE 17.4. *Parameters of Tokamak fusion reactors*

	JET	ITER
Torus radius, central point (m)	3.0	6.0
Vacuum chamber: width (m)	1.2	2.05
height (m)	3.0	6.0
Total reactor height (m)	11.3	27.6
Total reactor radius (m)	17.5	31.0
Plasma current (MA)	4-7	22
Toroidal field (T)	3.5	4.9
Power in (MW)	36	
Operation:		
ion temperature T (keV)	25	10-20
" (K)	2×10^8	$\sim 10^8$
ion density, n ($\times 10^{19}$ m^{-3})	4	25
pulse length/confinement time τ (s)	1.2 (25)	400
fusion product $n\tau T$ ($\times 10^{20}$ keV s m^{-3})	8-9	50
DT reactions/s	6×10^{17}	10^{21}
T-consumption (kg/d)†		0.43
DD reactions/s	1×10^{17}	
Power out (thermal MW)	2‡	1000

† At continuous operation. ‡ For about 2 s in DD reaction.

ions is an extremely difficult problem. Consequently, systems with injection of high energy neutral particles are under study. This could be accomplished through particle charge exchange, e.g.

$$D^+(\text{high energy}) + D(\text{low energy}) \rightarrow D(\text{high energy}) + D^+(\text{low energy}) \quad (17.42)$$

If all ions are removed magnetically, a beam of uncharged D-atoms (neutral beam injection, NBI) can enter the fusion volume. Another alternative being tested is high speed injection of small frozen D-T pellets into the hot plasma were they vaporize.

The withdrawal problem is even more difficult. Presently a shut down is necessary when large amounts of helium have been formed, after which the vacuum torus is purged and filled with a fresh D-T mixture. Considering the requirement of short interruptions in the energy production and the need to maintain an extremely high vacuum in the whole torus volume, a successful technical solution to this step is crucial.

(b) *Plasma confinement and heating.* The density must be increased to meet the Lawson criterion. This is achieved by increasing the magnetic field, which also leads to an ohmic heating of the plasma, though possibly not sufficient for ignition. Additional heating is required which possibly can be achieved by high frequency (ion cyclotron resonance) heating. Injection of deuterium/tritium ions of high kinetic energy is another (cf. (17.42)). After ignition further heating comes from the 3.5 MeV α-particles of reaction (17.17).

A magnetic field cannot, of course, increase indefinitely. When it has reached it maximum value, the machine must be shut down to allow the magnets to relax. The cycling time may be 3 – 10 minutes. The magnetic field goes to extremely high values, requiring superconducting magnets and extremely sturdy construction, as the high current ($\geq$ 30 000

A) through the magnet coils leads to a pressure of $>$ 1 ton cm^{-2}.

Particle injection, withdrawal, and heating lead to the emission of bremsstrahlung and synchrotron radiation of an energy much less than that corresponding to the fusion temperature. It is, therefore, lost by the plasma and absorbed in the walls of the vessel, which must be cooled. An additional difficulty is the heat insulation required between the very hot walls of the vacuum vessel ($\sim 1000^{\circ}$C) and the current carrying very cold super-conducting coils (at ~ 4.5 K).

(c) *Energy extraction and fuel cycle*. In the DT cycle 80% of the energy appears as neutron kinetic energy (14 MeV). Most steady state concepts involve the capture of this energetic neutron in a surrounding blanket containing lithium as a metal or salt (e.g. Li_2BeF_4) in which tritium is produced according to

$$^{6}\mathrm{Li}\ (7.4\%) + \mathrm{n} \rightarrow {}^{3}\mathrm{H} + {}^{4}\mathrm{He} \quad Q = 4.78\ \mathrm{MeV} \tag{17.43}$$

Neutrons reacting with the other Li-isotope yield two ^{4}He:

$$^{7}\mathrm{Li}\ (92.6\%) + \mathrm{n} \rightarrow 2\,{}^{4}\mathrm{He} \quad Q = 18.13\ \mathrm{MeV} \tag{17.44}$$

These reactions develop additional kinetic energy, which is converted into blanket heat. Most of the energy of the fusion process appears therefore in the hot blanket. If the blanket is in the form of molten lithium metal or salt, it can be pumped through a heat exchanger, which, in a the secondary circuit, produces steam for a turbine. Although the melting point of Li metal is only 186°C the Li temperature in the system will probably be around 1000°C. The tritium produced must be recovered for recycling as fuel.

The DT reactor needs several kg tritium as starting material. A likely technique involves the irradiation of a ^{6}Li-Al alloy in a high flux thermal fission reactor which produces both tritium and ^{4}He (17.43); These can be separated on the basis of their different vapor pressures, different permeability through palladium, or through their different chemical reactivities.

The first fusion reactors probably will use the DT-reaction, as the DD-reaction requires higher temperatures, Figure 17.5. The DT-reaction yields on the average 0.5 neutrons. Provided the blanket consists of only ^{6}Li, this produces 0.5 new T-atoms (per consumed T-atom); if the blanket also contains ^{7}Li, the yield of new T will be less. Therefore, the DT-fusion reactor must be fed continually with new tritium, produced in fission reactors. This demand will not be eliminated until the DD-fusion reactor comes into operation.

(d) *Construction material*. A major area of research is the proper choice of construction material, which should be strong, heat and radiation resistant, and have low neutron capture cross sections. However, materials testing will not be intensely tackled until ITER comes into operation. A preliminary materials choice could be the following, starting from the center of the plasma:

(1) A vacuum chamber of 10 cm stainless steel, on the inside lined with reinforced carbon shields to protect the steel. The chamber walls are water cooled. As the shielding erodes it has to be occasionally replaced by remote control.

(2) A water cooled blanket (and shield), ca. 1.5 m thick, made of vanadium alloy (e.g. V-15Cr-5Ti) and containing solid or liquid lithium. As much heat is produced, the lithium is used both for cooling and breeding and is pumped to heat exchangers for steam production followed by chemical treatment to recover the tritium. Cooling can also be achieved by He-gas, in which case the Li-system must be treated separately.

(3) A water cooled shield and thermal insulator, containing γ- and n-absorbing material.

(4) A liquid helium cooled superconducting magnet coil.

(e) *Health, environmental and economic aspects*. An operating reactor would contain several kilograms of tritium (1 kg of T_2 is about 4×10^{17} Bq of radioactivity) which presents a hazard corresponding to the noble gas fission products. However, tritium is more difficult to contain because of its ability to pass through many metals, especially at high temperatures. Moreover, tritium can exchange with hydrogen atoms in water, and thus become an ingestion hazard. Tritium is already a problem for fission reactors; for fusion reactors the problem is at least a factor of 1000 greater. Hence, the fusion reactor must be sealed extremely well against tritium leakage.

The structural material will be exposed to high radiation fields, causing radiation damage and induced radioactivity. The preferred material at present seems to be reinforced carbon, special steel and vanadium. Thus, considerable amounts of ^{49}V ($t_{1/2}$, 330 d), and possibly also some very long-lived ^{53}Mn, are formed. This induced activity will be a maintenance hazard, requiring remote control systems. However, compared to a fission reactor of similar size, the fusion reactor will contain less total radioactivity, and (of special importance in waste disposal) be free of long-lived α-activities.

A safety aspect, which has not been thoroughly studied, is the rapidly changing strong magnetic field (1 T s^{-1}), which will put great stress on the coils and structural material. The effects of such high fields on the operators are unknown.

The CTR's appear more complicated than the fission reactors. The cost of the raw material for the two energy systems — ^2H- and ^6Li-enrichment, and T-production (~ 50% by irradiation in fission reactors), compared to U-production and enrichment — are probably rather similar, and is a minor factor in the net economy of both systems. Waste handling will probably be cheaper for the fusion system. On balance, it is unlikely that fusion energy will become cheaper then fission energy. As long as the DT-reaction is used, fuel supply will be limited by the availability of Li. Further, considering that with fission breeders the uranium energy resources are sufficient for several centuries, there seems to be little incentive for the industry to engage in a rapid development of CTR's, although a steady, well planned research is expected to continue on an international basis as fusion energy using the DD-reaction promises to be the long term answer to the world's energy needs.

17.9. Exercises

17.1. (a) What is the most probable kinetic energy of a hydrogen atom at the interior of the sun ($T = 1.5 \times 10^7$ K)? (b) What fraction of the particles would have energies in excess of 100 keV?

17.2. Consider a power reactor in which microspheres ($r = 0.3$ mm) of frozen 1:1 T-D mixture (density 170 kg m^{-3}) are fused by laser irradiation. The laser compresses the spheres to $N_v = N_v^o 10^4$, where N_v^o is the number of atoms per m^3 at ordinary pressure, and also heats it to a temperature corresponding to almost 20 keV. The energy developed through the T-D fusion reaction leads to expansion of the spheres, which occurs with the velocity of sound ($v_s = 10^8$ m s^{-1}). This leads to no more than 25% of the particles fusing. What power is produced if the fusion micro-explosions occur at a rate of 30 per s?

17.3. If the deuterium in sea water is extracted and used to produce energy through reaction (17.12), what amount of gasoline (heat of combustion is assumed to be 35 MJ l^{-1}) would be equivalent to 1 liter of sea water?

17.4. What amount (kg) of hydrogen is consumed per second by the sun in the fusion reaction 17.5 in Table 17.1? The solar constant (energy flux at earth's orbit) is 1.353 kW m^{-2} and the earth's average distance to the center of the sun is 149 599 000 km.

17.5. Deuterium is to be injected into a fusion reactor at a density of 10^{20} D^+ and 10^{20} e^- m^{-3} and an energy of 100 keV. How much of the deuterium must fuse to compensate for the ionization and injection energy? The ionization energy of the deuterium atom is 13 eV.

17.6. In a water power station with a fall height of 20 m and a water flow of 500 m^3 s^{-1}, the electric power output at 100% efficiency can be calculated. If the heavy water in the fall could be extracted and converted in a fusion reactor according to (17.18) with a 25% efficiency, which of the two power sources would yield more energy?

17.10. Literature

Cosmology

G. GAMOW and C. L. CRITCHFIELD, *The theory of atomic nucleus and nuclear energy sources*, The Clarendon Press, 1949.
E. M. BURBIDGE, G. R. BURBIDGE, W. A. FOWLER and F. HOYLE, Synthesis of the elements in stars, *Rev. Mod. Phys.*, **29** (1957) 547.
H. CRAIG, S. L. MILLER and G. J . WASSENBURG (Eds.), *Isotopic and Cosmic Chemistry*, North-Holland, 1963.
Abundances of the elements in the universe, Landolt-Börnstein Physical Tables, New Series VI/1, 1965.
D. D. CLAYTON, *Principles of Stellar Evolution and Nucleosynthesis*, McGraw-Hill, 1968.
V. TRIMBLE, The origin and abundances of the chemical elements, *Rev. Mod. Phys.*, **47** (1975) 877.
J. E. ROSS and L. H. ALLER, The chemical composition of the sun, *Science*, **191** (1976) 1223.
S. WEINBERG, *The First Three Minutes*, Basic Books Inc., New York 1977.
J. RYDBERG and G. CHOPPIN, Elemental evolution and isotopic composition, *J. Chem. Ed.*, **54** (1977) 742.
The Cambridge Encyclopedia of Astronomy, Trewin Coppelstone Publ. Ltd, London 1977.
Landolt-Börnstein, New Series VI, Astronomy and Astrophysics Vol. 2a-c, Springer Verlag, 1981-1982.
P. K. KURODA, *The Origin of the Chemical Elements*, Springer Verlag, 1982.
B. MASON and C. B. MOORE, *Principles of Geochemistry*, J. Wiley & Sons, 1982.
H. D. HOLLAND, *The chemical evolution of the atmosphere and the oceans*, Princeton Univ. Press, 1984.
H. KARTTUNEN, P. KRÖGER, H. OJA, M. POUTANEN and K. J. DONNER, *Fundamental Astronomy*, Springer Verlag, 1987.
G. O. ABELL, D. MORRISON and S. C. WOLFF, *Exploration of the Universe*, Saunders College Publishing, 5th Ed., 1987.
P. A. COX, *The Elements*, Oxford Univ. Press, 1989.

Controlled fusion

M. J. MONSLER, J. HOVINGH, D. L. COOK, T. G. FRANK and G. A. MOSES, An overview of inertial fusion reactor design, *Nucl. Techn. Fusion*, **1**, July 1981, 302.
J. R. ROTH, The Impact of Engineering Constraints on the Feasibility of Advanced Fuel Fusion Reactors, *Nucl. Techn. Fusion*, **2** (1982) 29.
P. A. ERTAUD, Fusion thermonucleaire controlee – la grande illusion, *RGN*, Mai-Juin 1985, 242.
R. W. CONN, V. A. CHUYANOV, N. INOUE and D. R. SWEETMAN, The International Thermonuclear Experimental reactor, *Sci. Am.*, April 1992, 75.
J. G. CORDEY, R. J. GOLDSTON and R. R. PARKER, Progress Toward a Tokamak Fusion Reactor, *Physics Today*, Jan. 1992, 22.